

Understanding the phonon spectrum of plutonium

Walter A. Harrison

Los Alamos National Laboratory and Department of Applied Physics, Stanford University, Stanford, California 94305, USA

(Received 29 September 2003; published 30 March 2004)

The recently observed vibration spectrum of face-centered-cubic plutonium is interpreted in terms of a simple inclusion of electron correlations in a Friedel Model of the density of f -electron states, and an empty-core pseudopotential treatment of the three free electrons per atom. This model has given reasonable accounts of the volume-dependence of the total energy and of the experimental density of electronic states. It yields a volume-dependent energy, plus a two-body central-force interaction $V(d)$ between atoms, which enters the vibration spectrum only through the two parameters, $V^{(1)} = d\partial V/\partial d$ and $V^{(2)} = d^2\partial^2 V/\partial d^2$, evaluated at the nearest-neighbor distance. Using existing parameters yields the three elastic constants in crude accord with experiment but peak vibrational frequencies too low and an instability against shear modes in the [111] and [110] directions. Moderate scaling of the two parameters brings the vibration spectrum into reasonable accord. It also produces the strong fluctuation in the [110] T_1 mode, suggesting it is not from Kohn anomalies, which are absent from the model.

DOI: 10.1103/PhysRevB.69.113106

PACS number(s): 71.28.+d, 63.20.Dj, 62.20.Dc

I. INTRODUCTION

Wong, Krisch, Farber, Occelli, Schwartz, Chiang, Wall, Boro, and Xu¹ have recently given the remarkable first experimental vibration spectra of δ -plutonium, shown in Fig. 1. It was in quite good accord with a spectrum calculated by Dai, Savrasov, Kotliar, Migliori, Ledbetter, and Abrahams² using Dynamical Mean Field Theory (DMFT), as also seen in Fig. 1. Soon after, a spectrum was deduced from a phonon density of states from inelastic neutron scattering by McQueeney, Lawson, Migliori, Kelley, Fultz, Ramos, Martinez, Lashley, and Vogel.³ The calculation by Dai *et al.*, also reproduced the strong experimental elastic anisotropy of plutonium. An important feature of DMFT is that it reduces the effect of the interatomic interactions between neighboring f -states in comparison to Local Density Theory. We have proposed⁴ a very much simpler and more direct way of incorporating the effects of strong electron correlations, and used it to calculate the volume-dependent total energy of the actinides⁴ and their electronic properties.⁵ We use it here to shed light on the remarkable elastic and vibrational properties of plutonium.

The basis of the method is simplifying the local-density-approximation (LDA) aspects of the f -shell problem to a single parameter, the width W_f of the f -band, so that an exact solution of a correlated two-electron problem can be generalized to the metal. This misses some consequences of the full band structure, such as Kohn anomalies, but becomes so simple that it is much easier to see the origin of interesting effects.

II. METHOD

Already in 1982 Harrison and Wills⁶ had seen that simple metals could be described in terms of two-body central-force interactions between ions, obtained with an empty-core pseudopotentials (of core radius r_c) using Fermi-Thomas screening [parameter $\kappa = (4e^2k_F m/\pi\hbar^2)^{1/2}$]. For ions of valence Z , separated by distance d , it was given by (e.g., Ref. 4, p. 490).

$$V_{fe}(d) = \frac{Z^2 e^2 \cosh^2 \kappa r_c e^{-\kappa d}}{d}. \quad (1)$$

There was an additional volume-dependent energy [Eq. (1) is a purely repulsive interaction], which did not enter when Harrison and Wills used this form to calculate the vibration spectrum (at constant volume) of the simple metals and, from the spectrum, the elastic constants.

In the actinides there are $Z=3$ electrons per ion which may be regarded as free,⁴ and Eq. (1) used to evaluate their contribution to the energy change as ions are displaced. In addition, there is a partly-filled f -band, which in LDA would have some band width W_f , which we describe in a Friedel Model as a constant density of states $14/W_f$ over a range W_f . Then if there is an on-site Coulomb repulsion U_f between f -electrons (relative to the interaction when one is in an s -state), the contribution to $V(d)$ due to the coupling between f -states obtained by dividing the total f -shell energy (given in Ref. 4, p. 620, but written in terms of the fcc spacing d rather than the atomic-sphere radius r , $4\pi r^3/3 = d^3/\sqrt{2}$, as suggested on p. 624 of Ref. 4) by six, the number of nearest-neighbor interactions per ion. It is

$$V_f(d) = -\frac{Z_f(1-Z_f/14)}{12} \left(\sqrt{\left(\frac{\hbar^2(6.49r_f)^5}{md^7} \right)^2 + U_f^2 - U_f} \right) + Z_f \frac{\hbar^2(3.98r_f)^{10}}{6md^{12}}. \quad (2)$$

For plutonium, $Z_f=5$, $U_f=4.61$ eV, and $r_f=0.58$ Å (from Ref. 4, p. 605). This contribution to the interatomic interaction is shown as “ f -shell” in Fig. 2. The interaction from the three free-electrons per atom was obtained from Eq. (1), with the core radius $r_c=0.69$ Å (also Ref. 4, p. 605) adjusted such that the total energy, including volume-dependent-terms from the free-electron energy, was minimum at the α -plutonium spacing). The resulting interatomic interaction, shown as “Total” in Fig. 2, can be used to cal-

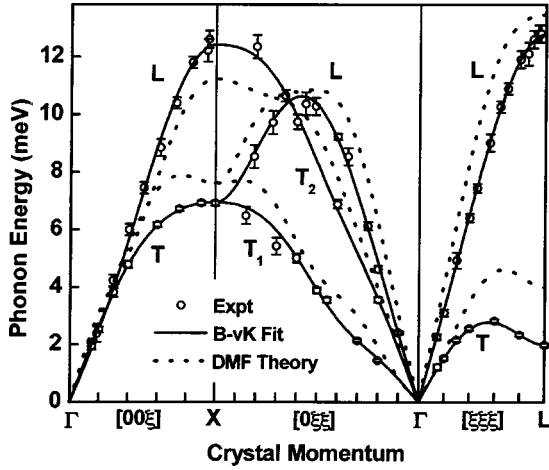


FIG. 1. The phonon dispersion along high symmetry directions in δ -plutonium, obtained by inelastic x-ray scattering by Wong *et al.* (Ref. 1), shown as circles, and fit (solid curves) with a fourth-nearest-neighbor Born-von Kármán model. Also shown are the theoretical results (dashed lines) obtained by Dai *et al.* (Ref. 2) using DMFT. Reproduced from Ref. 1. Reprinted (abstracted/excerpted) with permission from Joe Wong *et al.*, Science **301**, 1078 (2003). Copyright 2003 AAAS. URL: <http://www.sciencemag.org>

culate changes in energy as the atoms are rearranged at the constant volume of δ -plutonium, as done for simple metals by Harrison and Wills.⁶

We include only nearest-neighbor interactions since the r_c was fit including only nearest neighbors, and the f -shell contribution is clearly negligible at the second-neighbor distance of 4.6 Å. The vibration spectrum in fact depends only upon the first and second derivatives of $V(d)$ at the nearest-neighbor distance of $d = 3.275$ Å in plutonium. These derivatives are obtained adding Eqs. (1) and (2) and are conveniently written as $V^{(1)} = d\partial V/\partial d = -1.61$ eV and $V^{(2)} = d^2\partial^2 V/\partial d^2 = 7.66$ eV.

In an analysis⁷ following that in Ref. 4 we adjusted the parameters in an effort to understand the structural transformations in plutonium. We choose not to make those shifts here and proceed with the initial parameters.

III. SPECTRUM

In the face-centered-cubic structure, with one ion per primitive cell, the displacement of the ion initially at \mathbf{r}_j can be written $\mathbf{u}_j = \mathbf{u}_0 \cos(\mathbf{q} \cdot \mathbf{r}_j - \omega t)$ in terms of the amplitude vector \mathbf{u}_0 for a mode of wave number \mathbf{q} . The calculation of change in force on the central ion due to relative motion of a neighbor is a little tricky, but was carried out by Straub,⁸ and the result is clear and understandable. At $t = 0$ the force on an atom initially at $\mathbf{r}_j = 0$ due to interaction with an atom at \mathbf{d} has a component along \mathbf{u}_0 of

$$F = [(1/d)\partial V/\partial d \sin^2 \theta + \partial^2 V/\partial d^2 \cos^2 \theta] \times u_0 [\cos(\mathbf{q} \cdot \mathbf{d}) - 1] \quad (3)$$

if the angle between \mathbf{u}_0 and \mathbf{d} is θ . The component of displacements along \mathbf{d} has a $\cos^2 \theta$ and $\partial^2 V/\partial d^2$ as expected,

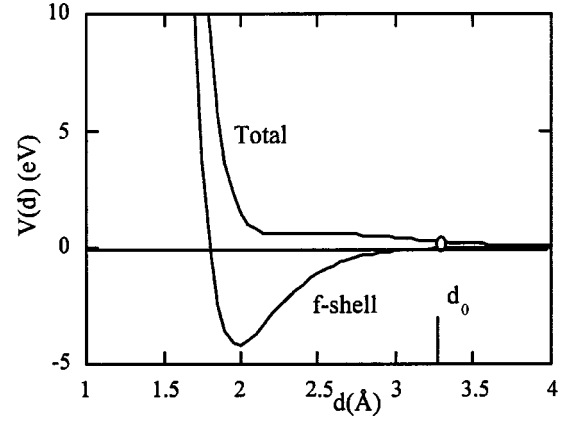


FIG. 2. The interatomic interaction between plutonium atoms arising from the f -shells, and obtained from Eq. (2), and the total obtained by adding the free-electron part from Eq. (1), all with parameters given earlier. The only numbers which enter the calculation of phonon spectra, based upon nearest neighbor interactions, are the slope and second derivatives of the curves at the observed spacing, indicated by the circle.

with $u_0[\cos(\mathbf{q} \cdot \mathbf{d}) - 1]$ giving the difference in displacement of the two atoms. This is in addition to the force $-\partial V/\partial d$ without displacement, which cancels when summed over all neighbors in the undistorted lattice. However, for displacements transverse to \mathbf{d} the rotated force has a component parallel to \mathbf{u}_0 proportional to $\sin^2 \theta$, the first term in Eq. (3). These last forces arise because there are additional volume-dependent terms in the energy, as for simple metals,⁶ and the Cauchy relations between the elastic constants will not be satisfied. The forces from Eq. (3) are to be added for all twelve neighbors, and the result equated to the atomic mass M times the acceleration, $\partial^2 \mathbf{u}_0/\partial t^2 = -\omega^2 \mathbf{u}_0$. Using also $\cos 2x - 1 = -2 \sin^2 x$ we may obtain for the phonon energy along the symmetry lines,

$$\begin{aligned} \hbar \omega_{L[100]} &= \sqrt{\hbar^2/Md^2} [8V^{(1)} + 8V^{(2)}]^{1/2} \sin(qd/\sqrt{8}), \\ \hbar \omega_{T[100]} &= \sqrt{\hbar^2/Md^2} [12V^{(1)} + 4V^{(2)}]^{1/2} \sin(qd/\sqrt{8}), \\ \hbar \omega_{L[110]} &= \sqrt{\hbar^2/Md^2} [(12V^{(1)} + 4V^{(2)})\sin^2(qd/4) \\ &\quad + 4V^{(2)} \sin^2(qd/2)]^{1/2}, \\ \hbar \omega_{T1[110]} &= \sqrt{\hbar^2/Md^2} [(12V^{(1)} + 4V^{(2)})\sin^2(qd/4) \\ &\quad + 4V^{(1)} \sin^2(qd/2)]^{1/2}, \\ \hbar \omega_{T2[110]} &= \sqrt{\hbar^2/Md^2} [(8V^{(1)} + 8V^{(2)})\sin^2(qd/4) \\ &\quad + 4V^{(1)} \sin^2(qd/2)]^{1/2}, \\ \hbar \omega_{L[111]} &= \sqrt{\hbar^2/Md^2} [4V^{(1)} + 8V^{(2)}]^{1/2} \sin(qd/\sqrt{6}), \\ \hbar \omega_{T[111]} &= \sqrt{\hbar^2/Md^2} [10V^{(1)} + 2V^{(2)}]^{1/2} \sin(qd/\sqrt{6}). \quad (4) \end{aligned}$$

The factor $\hbar^2/Md^2 = 1.623 \times 10^{-6}$ eV for Pu_{238} .

Note that $V^{(1)}$ is negative and if its magnitude is greater than $V^{(2)}/5$ the frequencies of the transverse [111] modes are

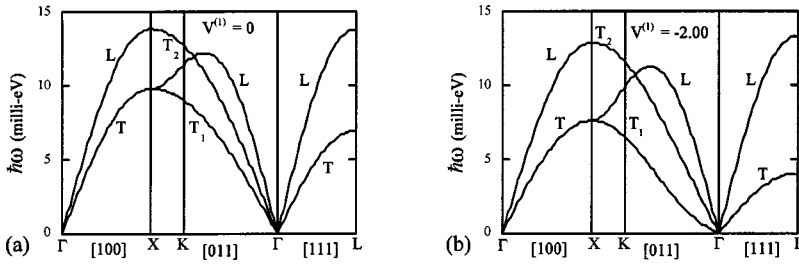


FIG. 3. The vibration spectrum from Eq. (4), with $V^{(2)}$ adjusted from 7.66 to 15 eV. In (a) $V^{(1)}$ is taken to vanish, but in (b) it is adjusted from our predicted -1.61 to -2 eV, still small enough to stabilize the lattice.

imaginary; the crystal is unstable against that entire branch. For the $V^{(1)} = -1.61$ eV and $V^{(2)} = 7.66$ eV given above, the system is just barely unstable against this mode. By taking the small- q limit we further see that if the magnitude of $V^{(1)}$ is greater than $V^{(2)}/7$, the low-frequency T_1 modes in the $[110]$ direction become unstable. We may also immediately evaluate the peak frequencies to see that they correspond to 8.9 and 9.1 meV for the $[100]$ and $[111]$ directions, respectively, rather than the 12 and 13 meV seen in Fig. 1. Our initial parameters are clearly not successful.

However, we may scale up $V^{(2)}$ by a factor of 2 to 15 eV, keeping $-V^{(1)}$ less than one-seventh of that value to obtain a reasonable spectrum. In Fig. 3(a) we have done that, taking $V^{(1)} = 0$. This gives the universal form for a fcc lattice for a radial, nearest-neighbor spring constant. In Fig. 3(b) we have included a $V^{(1)}$ of -2 eV, of larger magnitude than our prediction but smaller magnitude than $-V^{(2)}/7 = -2.14$ eV, making all modes stable. We could have interpreted this adjustment as changes in the two parameters of the theory, r_c and r_f [e.g., $r_c = 0.67$ Å, $r_f = 0.40$ Å yields $V_c^{(1)} = -2$ eV, $V_c^{(2)} = 15$ eV] but we found those parameters very sensitive to the $V^{(1)}$ and $V^{(2)}$ and we postpone such adjustment until we consider a more extensive set of properties.

This of course lowers the $[111]$ transverse mode, but cannot produce the dropping of the frequencies near L which is seen in Fig. 1 without more distant neighbors included. This drop presumably arises from a Kohn anomaly. It is quite interesting that it also introduces a droop in the $[110]$ T_1 mode which is quite reminiscent of that observed in the experiment, suggesting that the droop does *not* arise from such a Kohn anomaly. Our peak frequencies, 12.9 meV at X and 13.4 meV at L are only slightly higher than the experimental peaks. Figure 3(b) provides a qualitative agreement to the experimental curves with two parameters, not so far from our predicted values. At the same time two parameters cannot provide a good quantitative fit. Note that the experimental slopes of the two $[100]$ spectra at Γ are almost the same, but the values at X differ by almost a factor of 2, which are not consistent with both branches being proportional to $\sin(qd/\sqrt{8})$ according to Eq. (4).

The predicted instabilities which occur when $V^{(1)}$ becomes too large are peculiar ones. A way of visualizing that of the $[111]$ transverse mode, is to imagine a $V(d) = A/d^n$, rather than that from Eqs. (1) and (2). It yields $V^{(1)}/V^{(2)} = -1/(n+1)$ and says that this transverse mode will become unstable (with only nearest-neighbors included) when $n < 4$. It is true that with such a soft $V(d)$ the energy from the three neighbors in the next plane is a maximum at the center and therefore unstable, while not if $n > 4$. Of course, with such a

soft potential one can not neglect more distant neighbors, but with our potential we perhaps can. The instability has arisen because the f -shell contribution reduces the curvature by 35% while only lowering the magnitude of the slope by 15%. It has a large effect also for the T_1 mode in the $[110]$ direction.

IV. ELASTIC CONSTANTS

We may also obtain the elastic constants from the speeds of sound for the various modes. The squared speed of sound of the longitudinal mode in the $[100]$ -direction is $v_s^2 = c_{11}/\rho$, with $\rho = M\sqrt{2}/d^3$ the density. For the transverse mode in the $[100]$ direction it is $v_s^2 = c_{44}/\rho$, and for the T_1 mode in the $[110]$ direction it is $v_s^2 = (c_{11} - c_{12})/2\rho$. Equating these to the speeds obtained from Eq. (4) yields

$$c_{11} = (\sqrt{2}/d^3)(V^{(1)} + V^{(2)}) = 0.84 \times 10^{12} \text{ ergs/cm}^3,$$

$$c_{12} = (\sqrt{2}/d^3)(-\frac{5}{2}V^{(1)} + \frac{1}{2}V^{(2)}) = 0.81 \times 10^{12} \text{ ergs/cm}^3, \quad (5)$$

$$c_{44} = (\sqrt{2}/d^3)(\frac{3}{2}V^{(1)} + \frac{1}{2}V^{(2)}) = 0.29 \times 10^{12} \text{ ergs/cm}^3,$$

with the numerical values (note $10^{12} \text{ ergs/cm}^3 = 1 \text{ Mbar} = 100 \text{ GPa}$) obtained with the parameters $V^{(1)} = -2$ eV, $V^{(2)} = 15$ eV used for Fig. 3(b). This is in quite poor agreement with the experimental values⁹ of 0.36, 0.27, and 0.34, all times $10^{12} \text{ ergs/cm}^3$. Our initial predictions of $V^{(1)} = -1.61$ eV, $V^{(2)} = 7.66$ eV may do better at 0.39, 0.51, and 0.09 but they led to a negative shear constant $(c_{11} - c_{12})/2$ and thus an instability. Also we could never with Eq. (5) obtain a c_{44} comparable to c_{11} as observed, and seen in the $[100]$ spectrum.

Without the terms in $V^{(1)}$ we would have obtained $c_{44} = c_{12}$, the Cauchy relation, with both half of c_{11} . Fitting $V^{(1)}$ and $V^{(2)}$ to c_{11} and c_{12} would also yield a c_{44} a factor of 2 too small. The predicted constants do show the strong anisotropy of the two shear constants, $(c_{11} - c_{12})/2$ and c_{44} , giving a ratio of 1 to 19, compared to the experimental ratio of 1 to 8.

An important feature of this fit to the spectrum, in contrast to the Born-von Kármán fit of Fig. 1, is that if we write it in terms of r_c and r_f values we can immediately obtain the dependence of the parameters upon volume, needing only to add a $V^{(3)} = d^3 \partial^3 V / \partial d^3$ obtainable from the theory. Then the Grüneisen constants for each mode can be obtained and the various thermal properties calculated, and the theory even extended to alloys. Such an effort is currently under way.

- ¹Joe Wong, Michael Krisch, Daniel L. Farber, Florent Occelli, Adam J. Schwartz, Tai-C. Chiang, Mark Wall, Carl Boro, and Riquing Xu, *Science* **301**, 1078 (2003); see also commentary by Gerard H. Lander, *ibid.* **301**, 1057 (2003).
- ²X. Dai, S. Y. Savrasov, G. Kotliar, A. Migliori, H. Ledbetter, and E. Abrahams, *Science* **300**, 953 (2003).
- ³R. J. McQueeney, A. C. Lawson, A. Migliori, T. M. Kelley, B. T. Fultz, M. Ramos, B. Martinez, J. C. Lashley, and S. Vogel (unpublished).
- ⁴Walter A. Harrison, *Elementary Electronic Structure* (World Scientific, Singapore, 1999).
- ⁵Walter A. Harrison, *Phys. Rev. B* **68**, 075116 (2003).
- ⁶W. A. Harrison and J. M. Wills, *Phys. Rev. B* **25**, 5007 (1982), also described in Ref. 4, pp. 489ff.
- ⁷Walter A. Harrison, *Phys. Rev. B* **64**, 235112 (2001).
- ⁸Galen K. Straub, Los Alamos Technical Report No. LA-13193-MS (1996).
- ⁹H. M. Ledbetter and R. L. Moment, *Acta Metall.* **24**, 891 (1976).